Chin. J. Astron. Astrophys. Vol. 7 (2007), No. 2, 317–324
(*http://www.chjaa.org*)

Chinese Journal of
Astronomy and
Astrophysics

Eclipses and Occultations of Galilean Satellites Observed at Yunnan Observatory in 2003 *

Qing-Yu Peng[1,3] and Benoît Noyelles[1,2]

[1] Department of Computer Science, Jinan University, Guangzhou 510632; *pengqy@pub.guangzhou.gd.cn*
[2] Institut de mécanique céleste et de calcul des éphémérides - Observatoire de Paris, UMR 8028 du CNRS, 77 avenue Denfert-Rochereau, F-75014 Paris, France
[3] Joint Laboratory for Optical Astronomy, Chinese Academy of Sciences, Kunming 650011

Received 2006 June 1; accepted 2006 October 10

Abstract We describe and analyze observations of mutual events of Galilean satellites made at the Yunnan Observatory in February 2003 from CCD imaging for the first time in China. Astrometric positions were deduced from these photometric observations by modelling the relative motion and the photometry of the involved satellites during each event.

Key words: planets and satellites: individual: Jupiter — astrometry — eclipse — occultation

1 INTRODUCTION

When the Earth goes through the common orbital plane of the Galilean satellites (i.e., when the jovicentric declination of the Earth becomes zero) mutual occultations occur. Similarly, when the Sun goes through the common orbital plane of the Galilean satellites (i.e., when the jovicentric declination of the Sun becomes zero) mutual eclipses occur (see Fig. 1, originally from the website *http://www.imcce.fr*). Mutual occultations and mutual eclipses are simply known as mutual events or mutual phenomena.

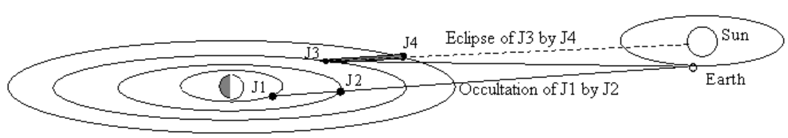

Fig. 1 Definition of the mutual events. J1-Io partially disappears behind J2-Europa for a terrestrial observer, while J3-Ganymede is less visible than usual, because of J4-Callisto's shadow.

During a mutual event, a record of the photometry of the two involved bodies shows a light flux drop, as can be seen in Figure 2. These photometric variations of the bodies can be used to obtain an astrometric position with a high accuracy. In fact, observations of the mutual events are among the most accurate ground-based observations from an astrometric point of view, see e.g., Lieske (1998) and Jacobson (2004).

Such mutual events happen every 6 years for the Galilean satellites, 15 years for the Saturnian and 42 years for the Uranian ones. Since 1979 the IMCCE (Paris Observatory, France) has systematically organized worldwide campaigns of observations of these events with a growing success. Until now, five observational

* Supported by the National Natural Science Foundation of China.

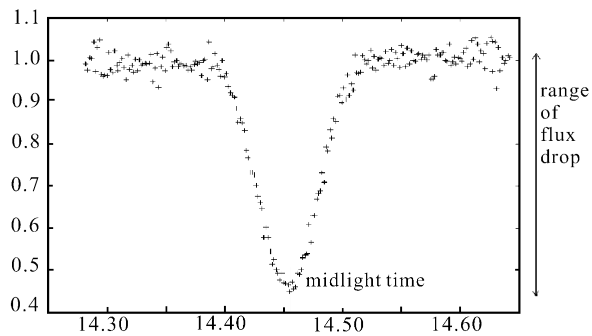

Fig. 2 An example of lightcurve of mutual event (eclipse of J-2 Europa by J-4 Callisto observed on 2003 February 20, at the Yunnan Observatory). Here the x-axis is the UTC decimal hour, and the y-axis the light flux normalized to 1 outside of the event. One can see the range of flux drop, i.e., the biggest light loss during the event, and the midlight time, which is the time corresponding to the flux drop.

campaigns of the mutual events of Galilean satellites as well as two of Saturnian satellites have been organized.

In 2003, the mutual events of Galilean satellites predicted by Arlot (2002) were observed at Yunnan Observatory. More precisely, eight observations were performed in February 2003. We present here an introduction of the observations and the astrometric reduction of the data.

2 OBSERVATIONS

For the 1-m telescope at the Yunnan Observatory ($102°47'.3$ E, $25°1'.5$ N and altitude 2000 m, IAU code 286), a scientific-type Princeton 1024×1024 CCD has routinely been in use since 1995. Table 1 gives the specifications of the telescope and its attached CCD chip. Usually, there is a choice of three CCD readout rates (50, 100 and 150 kHz).

Table 1 Specifications of Yunnan Observatory 1-m telescope and its attached CCD chip

Focal length	1300 cm
F-Ratio	13
Diameter of the primary mirror	100 cm
CCD field of view	$6'.4 \times 6'.4$
Size of each pixel	$24\,\mu\text{m} \times 24\,\mu\text{m}$
Size of CCD array (resolution)	1024×1024
Angular extent per pixel	$0''.37$

In order to obtain useful lightcurves, we set up special observing procedures. First, we chose the fastest readout mode (i.e., 150 kHz). Secondly, a window (1024×512) was opened on the imaging area of the CCD chip. A smaller window was not adopted for the reason that a reference object (usually another satellite) whose light is constant during the event was required. Moreover, we need to obtain the full image of Jupiter so as to be able to remove the positional effect of its halo on the satellites according to the methods presented in our former work (Peng et al. 2003). A keyboard rather than a mouse was used to speed the acquisition during the observations. The frequency was about one image every 5 or 6 s for our CCD camera. An I-type filter and an integration time of about 0.5 s were used for each CCD image. Because of the low sampling frequency, we had to choose some relatively long-duration mutual events so as to minimize the relative timing errors.

A GPS receiver was used for the time recording, and the time was displayed on a computer screen. Because the GPS receiver was not specially used for our observations, it allowed a time precision of 1 s. From the times of exposure of the first and last images noted at the time the exact time of each image was interpolated in the later processing. However, later we found there existed a problem because not all the images between the first and last were evenly acquired from the manual operations. In other words, there was a sampling error in the time of observations. Therefore, for the later lightcurves we recorded the beginning time of the exposure of each image by hand. Obviously, the technique of time-recording should be improved in future for such observations.

Because a CCD is a two-dimension receiver, the images can be conveniently processed by some image-processing techniques. Here, we tried to use our CCD to observe some near-Jupiter mutual events. In fact, we have developed an image-processing software for the general CCD astrometry of Jupiter and its Galilean satellites. Figure 3 shows the image before and after processing. Here, we fitted the edge of the planetary disk with an elliptic curve to obtain its center. Then the halo of Jupiter was removed by an abstraction according to the methods presented in Peng et al. (2003). After the pre-processing, the background near the target or the reference was evenly distributed, then the photometry for the occulted or eclipsed satellite and the reference satellite were measured according to Colas & Arlot (2002). Although dark counts and flat fields were usually performed, no corrections were made in practice for our CCD images, since nearly no effect was found according to our previous analysis (Peng & Tan 2005).

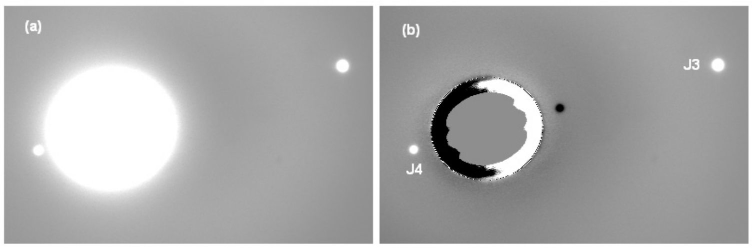

Fig. 3 Images before and after processing. (a) is the original one taken for the J1EJ4 on 2003 February 28 and (b) is the image after processing.

In February 2003, we observed eight lightcurves for mutual events. The details are given in Table 2, the observed dates, observational types (occultation or eclipse) and the involved satellites.

Table 2 Observed lightcurves at the Yunnan Observatory in 2003

year	mon	day	type	reference
2003	Feb	18	J4OJ3	J2
2003	Feb	18	J4EJ3	J4
2003	Feb	20	J4OJ2	J3
2003	Feb	20	J4EJ2	J4
2003	Feb	20	J1OJ2	J4
2003	Feb	27	J1OJ2	J4
2003	Feb	28	J1EJ4	J3
2003	Feb	28	J1OJ4	J2

In the column “Type”, “O” and “E” mean “Occultation” and “Eclipse”, respectively. The last column is the reference satellite for the light measurement.

In the case of an occultation, the light from both is observed, while in the case of an eclipse only the light of the eclipsed satellite is registered. Actually, a special event happened in the lightcurve of “J1EJ4” on 2003 February 28. As seen in Figure 4, before the end of the event, Callisto entered Jupiter’s shadow. By the way, for the last lightcurve on February 28 (“J1OJ4”), no obvious light variation was found, possibly because of its small amplitude of variation (see Fig. 5).

3 THE ASTROMETRIC REDUCTION

3.1 The Method

The reduction method we used is the same as that used by Vienne et al. (2003) to reduce the mutual events observed at Lille Observatory during the same campaign. We recall here its principles.

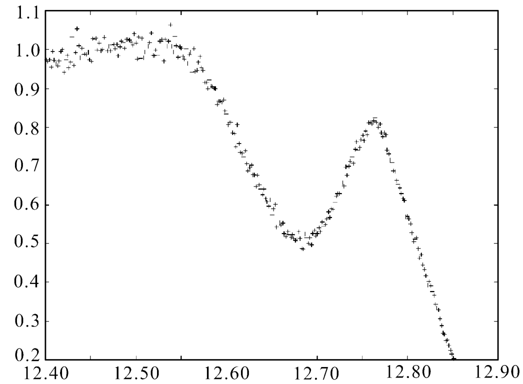

Fig. 4 Observation of the eclipse of Callisto by Io on February 28. We can see Callisto entering Jupiter's shadow before the end of the event.

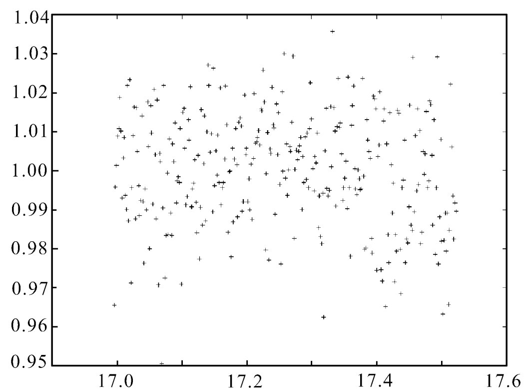

Fig. 5 Observation of the occultation of Callisto by Io on February 28. No event can be seen.

The first step is to model the event, which consists of two modelling, one is dynamical, one is photometric. For an occultation, the dynamical modelling assumes that, as seen by a terrestrial observer, the occulting satellite has a linear uniform motion relatively to the occulted one. For an eclipse, the assumption is the same when seen from the Sun's centre. Another difference between an eclipse and an occultation is the light time correction. For an occultation the light time correction depends on the distance between the observer and the two satellites, while for an eclipse, time correction is related to where the eclipsing satellite was and when it stopped the solar rays on the way to the eclipsed satellite. So the light time for the eclipsing satellite is longer than for the eclipsed one, as explained in Noyelles et al. (2003).

This dynamical modelling has three parameters: the midtime, the impact parameter and the relative velocity of the satellites on the celestial sphere. The impact parameter is the least distance between the two satellites projected on the celestial sphere (see Fig. 6), and the midtime is the time corresponding to this distance. It usually differs from the midlight time by a few seconds (see for instance Aksnes et al. 1986).

The photometric modelling is not so easy because, for an atmosphereless body, the diffusion of solar light by the surface is anisotropic. We modelled this diffusion by the Minnaert law (Minnaert 1961) considering that each satellite is seen as a disc darkened at the limb. More precisely, we modelled the diffusion of the solar light by a surface element with Equation (1)

$$\frac{I}{F}(i, e, \alpha) = B_0(\alpha)(\cos(i))^{k(\alpha)}(\cos(e))^{k(\alpha)-1}, \tag{1}$$

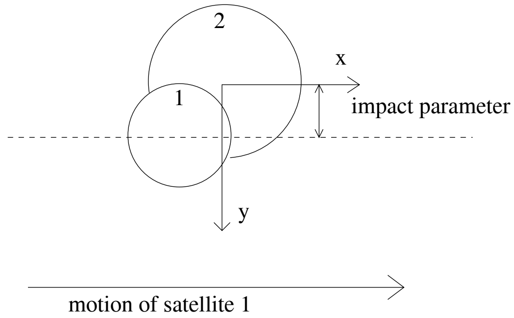

Fig. 6 Dynamical modelling of the event (from Noyelles et al. 2003). We assume the second satellite does not move and that the first one has a linear uniform motion.

where I is the reflected light per surface unit, πF the incident solar flux, i the light incidence angle, e the light emergence angle, α the phase angle, k the limb darkening, and B_0 the photometric parameter.

For an eclipse, we have to model the shadow of the eclipsing satellite, considering solar limb darkening. We estimated it using Hestroffer and Magnan's empiric law (1998). The light flux coming from a surface element of the solar disc is

$$I(\mu) = \mu^{\beta}, \tag{2}$$

where $\beta \sim$ –0.023+0.292λ^{-1}, if $\lambda^{-1} < 2.4\,\mu\mathrm{m}^{-1}$, $\beta \sim -0.507$+0.441λ^{-1}, if$\lambda^{-1} > 2.8\,\mu\mathrm{m}^{-1}$, λ being the wavelength in μm, $\mu = \sqrt{1-r^2}$, r the distance to the Sun's center, $R_{\odot} = 1$.

We thus computed the solar flux $i_{\odot}$ received by each point of the eclipsed satellite in the penumbra zone that is required to integrate Equation (2) over the solar disk. For this purpose, we obtained the following formula, with r in AU,

$$i_{\odot} = 1 - \frac{1}{2R_{\odot}^2}\left[\left(1-\frac{r}{R_{\odot}}\right)^{\frac{\beta}{2}}(r-R_{\odot})(2(r+R_{\odot})+\beta r)\right]_{r_0'}^{r_1'} + \frac{\beta^2+6\beta+8}{8\pi R_{\odot}^2}\int_{r_1'}^{r_2'} r\left(1-\frac{r}{R_{\odot}}\right)^{\frac{\beta}{2}}\Psi(R_1,r,R)dr, \tag{3}$$

where R_1 is the radius of the first satellite, r_0' =min[$R_{\odot}'$, max(0,$R-R_1$)], r_1' =min[$R_{\odot}'$, max(r_0', R_1-R)], $r_2' = \min(R_{\odot}', R+R_1)$, R is the distance between the second satellite and the center of the penumbra zone. $R_{\odot}'$ is the Sun's radius seen from the 2$^{\mathrm{nd}}$ satellite, as if the Sun and the 1$^{\mathrm{st}}$ satellite were at the same distance. Ψ is defined by

$$\Psi(R_1,r,R) = 2\arctan\left(\frac{\sqrt{r^2-a^2}}{a}\right), \tag{4}$$

where

$$a = \frac{r^2+R^2-R_1^2}{2R}. \tag{5}$$

Once the event is modelled, we fit the model to the observed lightcurve. For that, we use the Marquardt-Levenberg algorithm (Marquardt 1963) to obtain a non-linear least-squares fit. The parameters we fit are the midtime, impact parameter, relative velocity, limb darkening and, in case of an occultation, the ratio between the albedos of the two involved satellites. The dynamical initial condition of the fitting algorithm is taken from E5 ephemerides (Lieske 1998) used with the planetary theory SLP96, derived from VSOP87 (Bretagnon & Francou 1988). Our algorithm does not model an eclipse by the planet, so, in the case of the occultation of Callisto by Io on February 28 (Fig. 4), our model is adjusted only to the part of the observation not involving the eclipse by Jupiter. It has given good results anyway because we covered more than half of the event.

Table 3 Residuals obtained with Lieske's E5 theory

year	mon	day	sat	$\Delta\alpha \cos\delta$ arcsec	$\Delta\delta$ arcsec	f	o-c1 arcsec	o-c2 arcsec
2003	2	18.7450917	43	–0.1669358	–0.5108409	1	–0.175	–0.088
2003	2	18.8669868	43	–0.1779081	–0.5136461	2	0.000	0.078
2003	2	20.5124774	42	0.0216519	0.0691347	1	–0.158	0.064
2003	2	20.6022528	42	–0.1483601	–0.4406032	2	–0.029	0.038
2003	2	20.6589563	12	–0.0380041	–0.1196011	1	–0.154	0.128
2003	2	27.7413333	12	–0.0650795	–0.2080025	1	–0.164	0.120
2003	2	28.5282734	14	0.0522192	0.1493383	2	0.044	0.099

The second satellite is the reference. Frame 2 is heliocentric and frame 1 is geocentric. Time is UTC.

Table 4 Residuals obtained with Lainey's L1 theory

year	mon	day	sat	$\Delta\alpha \cos\delta$ arcsec	$\Delta\delta$ arcsec	f	o-c1 arcsec	o-c2 arcsec
2003	2	18.7450917	43	–0.1668618	–0.5108650	1	–0.168	–0.064
2003	2	18.8669868	43	–0.1778641	–0.5136613	2	0.007	0.100
2003	2	20.5124774	42	0.0216754	0.0691273	1	–0.108	0.054
2003	2	20.6022528	42	–0.1485132	–0.4405516	2	0.023	0.028
2003	2	20.6589563	12	–0.0379932	–0.1196046	1	–0.087	0.110
2003	2	27.7413333	12	–0.0650674	–0.2080063	1	–0.092	0.100
2003	2	28.5282734	14	0.0520435	0.1493996	2	0.035	0.109

Table 5 Photometric and dynamical parameters obtained after fit

event	k_1	p_2/p_1	k_2	impact param.	flux drop (%)
4o3182	0.5	6.200	0.700	1700 km	48.7
4e3182			0.490	2092 km	40.2
4o2202	0.5	3.160	0.580	230 km	59.0
4e2202			0.580	1789 km	53.6
1o2202	0.5	0.910	0.530	399 km	38.9
1o2272	0.5	0.887	0.700	700 km	34.8
1e4282			0.467	611 km	49.4

"4o3182" means "J4 occults J3 on February 18", p_1 and k_1 are albedo and limb darkening of the first satellite, p_2 and k_2 are the same for the second one. In the case of eclipse, since only the light from the second satellite is recorded, we have no information on the first satellite's photometry.

3.2 Results

Since no event is detected for the last observation (Fig. 5), we have only obtained seven astrometric positions, summarized in Table 3, while Table 5 gives some details about some parameters, photometric and geometric, deduced from the fit of the model to the observations. Figure 7 shows the observed lightcurves and the fit to the theoretical models.

The accuracy of the positions can be evaluated based on the last two columns of Tables 3 and 4, the differences between E5 and L1 (Lainey et al. 2004) predictions and our positions. We can see with Lieske's theory an average residual of 103 mas in right ascension, and 88 mas in declination, or about 300 and 250 km, while Lainey's theory seems to be more accurate, with an average residual of 74 mas in right ascension and 80 mas in declination (see Table 4).

4 DISCUSSION

The photometry of the Galilean satellites in the I-band is poorly known, and this complicates the photometric modelling of the satellites. Anyway, it is interesting to observe at this wavelength in order to contribute to a better knowledge of the photometry.

It is illustrated by the occultation of Europa by Callisto observed on February 20 (Fig. 7), which is an annular occultation. Our model gives a nearly flat curve during the annular time span, but the observed curve seems to be not so flat. The reason is there exists inhomogeneity in Europa's albedo at I-band. Such an observation can help us improve our knowledge of photometry.

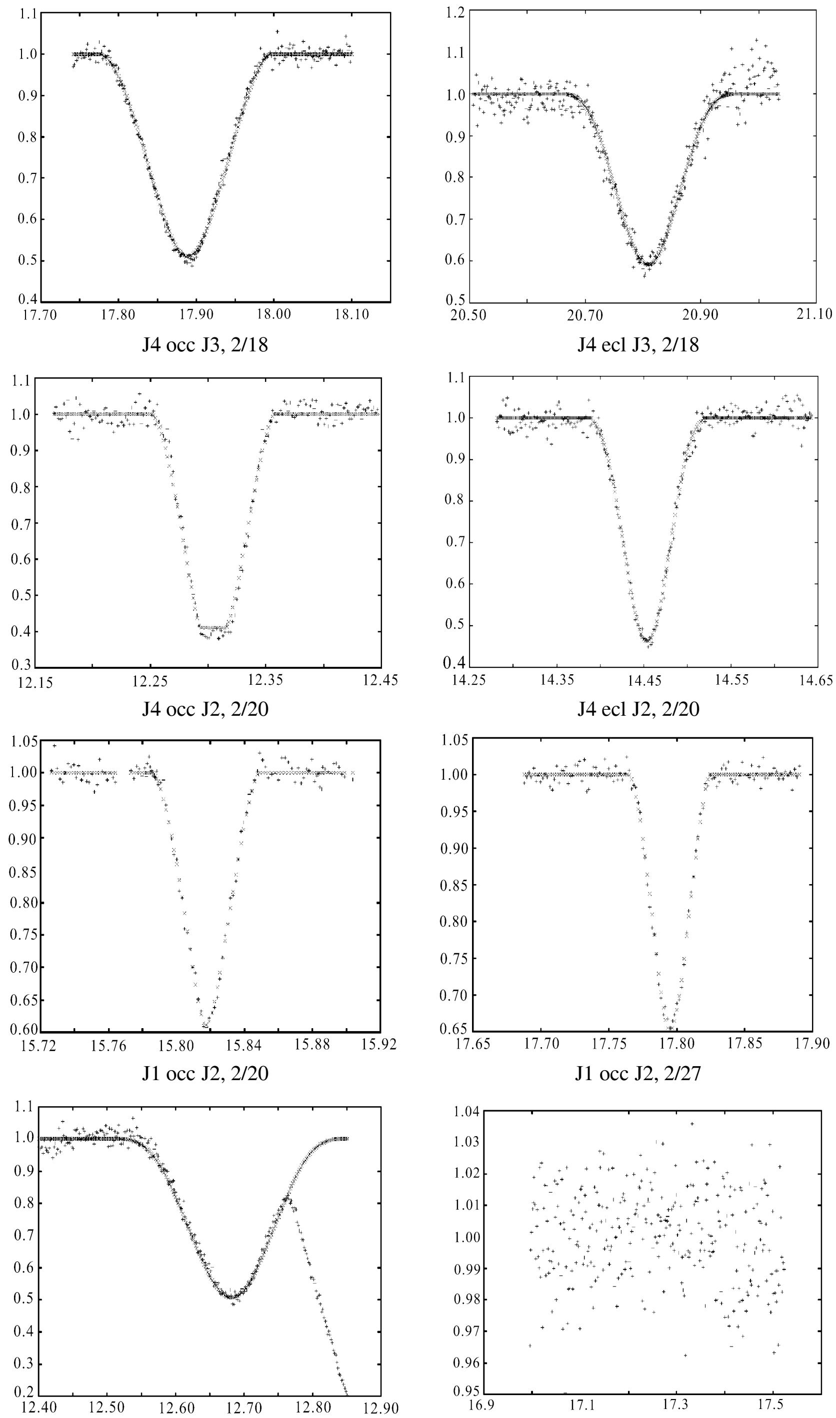

Fig. 7 Eight lightcurves we observed.

The fit to the eclipse of Callisto by Io on February 28 (Fig. 7) seems to give good results, while we did not observe the end of the event because of Jupiter's shadow. It would be very interesting on a future occasion to take the eclipse by the planet into account: it should improve the astrometric results.

The eclipse of Ganymede by Callisto on February 18 was also observed by Vienne et al. (2003) in the V-band at Lille Observatory. The position deduced can be seen in Table 6. We can see a very small difference of 0.3 s in the midtime (or about 3 km, taking account of Ganymede's mean motion) and of 65 km in the impact parameter. This gives us another way to evaluate the accuracy of the method. We cannot really compare the two flux drops because they have not been obtained at the same wavelength.

Table 6 Comparison with the astrometric result obtained by Vienne et al. (2003) at Lille Observatory

midtime (UTC)	impact parameter	flux drop	$\Delta\alpha\cos\delta$ arcsec	$\Delta\delta$ arcsec	obs site
$20^h48^m27.4^s$	2157 km	39.5%	−0.1833953	−0.5296350	Lille
$20^h48^m27.7^s$	2092 km	40.2%	−0.1778641	−0.5136613	Kunming

Finally we make a remark on the accuracy of the ephemerides. We have better residuals with Lainey's theory than with Lieske's. Lainey's theory seems to be more accurate, and this might be due to perturbations that Lieske did not take into account, like the oblateness of the four Galilean satellites. In the positions $(\Delta\alpha\cos\delta, \Delta\delta)$ we give in Tables 3 and 4, we can see very small differences, smaller than 1 mas. The reason is that the orientation of the line joining the two geometric centres of the involved satellites depends on the ephemerides, so a difference can be seen when we project the angular separation we derived from the impact parameter on the two axes α and δ (right ascension and declination). The two occultations of Europa by Io (on February 20 and February 27) give nearly the same residuals, and it can be a clue on the internal accuracy of our method, or of ephemerides. Since Lainey's theory seems to be more accurate than Lieske's, we advise the reader to use Table 4 rather than Table 3.

5 CONCLUDING REMARKS

It can be seen from our results that observations of mutual events are accurate ground-based observations. In the near future, their accuracy should be improved using albedo maps given by Galileo spacecraft, as already used by Vasundhara (2002). The next campaigns of mutual events will be in 2009 for the Galilean satellites, and in 2010 for Saturnian satellites. For the first time, mutual events of Uranian satellites can be observed between 2006 and 2010, and their predictions can be seen for instance from Christou (2005) or on the IMCCE web site http://www.imcce.fr.

Acknowledgements This research is under the support of National Natural Science Foundation of China (Grants 10273015, 10573008 and 10778617), IMCCE and the French Embassy in Beijing. The authors are indebted to Li Z. L. for his help during observations at Yunnan Observatory.

References

Aksnes K., Franklin F., Magnusson P., 1986, AJ, 92, 1436
Arlot J.-E., 2002, A&A, 383, 719
Bretagnon P., Francou G., 1988, A&A, 202, 309
Christou A. A., 2005, Icarus, 178, 171
Colas F., Arlot J.-E., 2002, Phemu03, TECHNICAL No.5
Hestroffer D., Magnan C., 1998, A&A, 333, 338
Jacobson R. A., 2004, AJ, 128, 492
Lainey V., Arlot J.-E., Vienne A., 2004, A&A, 427, 371
Lieske J. H., 1998, A&AS, 129, 205
Marquardt D. W., 1963, Journal of the Society for Industrial and Applied Mathematics, 11, 431
Minnaert M., 1961, in Planets and Satellites, eds. G. P. Kuiper, B. M. Middlehurst, The University of Chicago Press, p.213
Noyelles B., Vienne A., Descamps P., 2003, A&A, 401, 1159
Peng Q. Y., Han Y. B., Zhang C. L. et al., 2003, A&A, 401, 773
Peng Q. Y., Tan P. A., 2005, PNAOC, 2, 28
Vasundhara R., 2002, A&A, 389, 325
Vienne A., Noyelles B., Amossé A., 2003, A&A, 410, 343